

SEARCHING FOR THE MAGNETISED TIDAL DWARF GALAXIES IN HICKSON COMPACT GROUPS: HCG 26, 91, AND 96

BŁAŻEJ NIKIEL-WROCZYŃSKI^{1,2}

¹*Astronomical Observatory of the Jagiellonian University, ul. Orla 171, 30-244 Kraków, Poland*

²*Leiden Observatory, Leiden University, Oort Gebouw, PO Box 9513, NL-2300 RA Leiden, the Netherlands*

(Received June 24, 2019; Revised March 3, 2022; Accepted ZZZZ)

ABSTRACT

In this work, archive 1.4 and 4.86 GHz radio continuum data from the VLA were re-reduced and, together with the 1.4 GHz maps from the NVSS, investigated for the presence of a detectable, non-thermal continuum radio emission that could be associated with the TDG candidates in HCG 26, 91, and 96. Radio emission highly coincident with the optical and H_α emission maxima of the TDG candidate HCG 91i (estimated physical separation of less than 150 pc) was revealed. Should this emission be intrinsic to this object, it would imply the presence of a magnetic field as strong as 11–16 μG – comparable to that found in the most radio-luminous, star-forming dwarf galaxies of non-tidal origin. However, the star formation rate derived for this object using the radio flux is about two orders of magnitude higher, than the one estimated from the H_α data. Analysis of the auxiliary radio, ultraviolet and infrared data suggests that either the radio emission originates in a background object with an aged synchrotron spectrum (possibly a GHz-peaked source), or the SFR_{H_α} estimate is lower due to the fact that it traces the most recent star formation, while most of the detected radio emission originated when what is known as HCG 91i was still a part of its parent galaxy. The latter scenario is supported by a very large stellar mass derived from 3.6 and 4.5 μm data, implying high star formation in the past.

Keywords: galaxies:dwarfs – galaxies:groups:individual:HCG26 – galaxies:groups:individual:HCG91 – galaxies:groups:individual:HCG96 – galaxies:interactions – galaxies:magnetic fields

1. INTRODUCTION

The idea that small, self-gravitating entities can form out of the debris left by collisions and close passages of "normal" galaxies is a relatively new one, as it was proposed only about 60 years ago (Zwicky 1956). Zwicky analysed several aspects of the galactic interactions, e.g. the emergence of large tails, like that of the Leo Triplet, and on the basis of the disputed cases, came to a conclusion that defines the unique character of the tidal dwarf galaxies (TDG). However, albeit novel and (as turned out eventually) correct, Zwicky's idea did not gain much attention for more than 30 years. This was mainly due to the technical limitations of the that-day instruments that simply could not achieve sensitivity required to trace the weak light produced by the TDGs. In 1992, Mirabel et al. have announced a detection of such an object at the tip of the tidal tail of a famous merging galaxy pair, the Antennae. With this first discovery, the era of studying the TDGs has began.

The following years have brought a number of case studies of the TDGs, with examples of such objects detected eg. in Arp 245 (Brinks et al. 2004), in the Virgo Cluster (Duc et al. 2007), or in galaxy groups, like in M81 (Makarova et al. 2002), or in a number of Hickson Compact Groups (HCG, Hickson 1982), by Hunsberger & Zaritsky (1996). An important warning has also been formed: as only about 50% of the TDGs can survive for as long as the Hubble time (Bournaud 2010), and usually self-gravitation is only assumed, not proven, it is advisable to call these numerous detections as "candidates" (TDGc), being probable, but not certain, galaxies (Kaviraj et al. 2012). The growing database of supposed dwarfish galaxies with a tidal origin was calling for a statistical approach, in which typical parameters and traits of TDGs could be analysed. This was done by Kaviraj et al. (2012), who used the SDSS DR6 data (Abazajian et al. 2009) and built a sample of more than 3000 nearby (not further than $z = 0.1$) galaxy mergers that could possibly host TDG candidates. Inside these systems, as many as 405 candidate objects have been identified.

Studies on TDGs in galaxy groups constitute a separate and growing chapter in the history of their observations. The TDG formation efficiency drops down rapidly with the increasing density of the host systems (Kaviraj et al. 2012). They are much more scarce in galaxy groups than in pairs, and probably are eager to evolve differently. Complicated dynamics of the multi-galaxy systems increases the possibility that a newly born TDG candidate/progenitor will be ab-

sorbed in the subsequent galactic collisions (like it could have happened eg. in case of the Leo Triplet – Weżgowiec et al. 2012). Despite this impediment, studies carried out on the HCGs show that these systems can be quite abundant with TDG candidates. In particular, HCG 92 – the famous Stephan's Quintet (Stephan 1877) – has been concluded to host at least 20 candidate objects (Hunsberger & Zaritsky 1996), two of them (denoted SQ-A and SQ-B; Xu et al. 2003) being visible in multiple spectral regimes. A recent study by Eigenthaler et al. (2015) shows that other HCGs are also accompanied with TDG candidates, and some of these groups can host a significant number of them (eg. HCG 91).

When discussing the TDG candidates found in galaxy groups, two of them should be especially mentioned: SQ-A, and SQ-B which are located in the tidal tail of NGC 7319, a member galaxy of the Stephan's Quintet. What is special about these objects is that they emit in the radio continuum (Xu et al. 2003). This emission has a non-thermal character, and there are hints that it is partially polarised in case of the latter one (Nikiel-Wroczyński et al. 2013b), signifying the existence of a detectable magnetic field, probably at least ordered (if not genuinely regular), inside this objects. Albeit a possibility that the matter forming a TDG is magnetised is certainly not an exotic one – most of the spiral galaxies host relatively strong magnetic fields (Niklas 1995), and these are mostly spirals that serve as progenitors to TDG candidates (TDGc, Kaviraj et al. 2012) – SQ-A and SQ-B remain the single known examples of the magnetised TDGc so far. Hints for the radio emission from a TDGc in Leo Triplet (Nikiel-Wroczyński et al. 2013a) have turned out to be caused by a background source smeared by the large beam of the single-dish observations used in that study (Nikiel-Wroczyński et al. 2014). Attempts to detect radio emission in other TDGc – eg. in the Antennae, K. Chyży, (priv. comm.) – have turned out to be fruitless so far.

In general, detection of the magnetic field inside, or around a TDGc should not be very surprising. Conditions favourable for their formation, like the presence of spiral galaxies, or effective processes of star forming, are preferable for the magnetic fields to be amplified, too. However, magnetic fields found in dwarfish galaxies are usually weaker, than those found in the spiral ones: whereas the median strength of the magnetic field in spiral galaxies is $9 \pm 1.3 \mu\text{G}$ (Niklas 1995), values as low as a few microgauss are usually reported for the dwarf ones

(see Chyży et al. 2011 and references therein). Strong magnetic fields are found only in the so-called starburst dwarf galaxies (eg. NGC 1569, Kepley et al. 2010, or NGC 4449, Chyży et al. 2000), and can be considered an exception to this rule. Alas, the sample of the studied TDG candidates is still too scarce to investigate the role and general properties of the magnetic fields inside them, and it is desirable to enlarge it.

In this paper, the results of investigating the radio maps of those HCGs that have been marked by Eigenthaler et al. (2015) as possible hosts of TDG candidates are presented. Archive radio data from the Very Large Array (VLA), and the NRAO VLA Sky Survey (NVSS; Condon et al. 1998) were analysed for each of these systems, revealing radio emission possibly associated with HCG 91i both at 1.4 and 4.86 GHz. The paper is organised as follows: Sec. 2 contains the basic information on the data used, as well as information about their processing, Sec. 3 describes the radio maps of the studied groups and relates them to the list of TDG candidates compiled by Eigenthaler et al. (2015). Sec. 4 discusses the arguments in favour and against possible connection between the detected radio emission and HCG 91i, as well as evaluates different explanations for the detected signal, while Sec. 5 summarises the findings of this article.

2. OBSERVATIONS AND DATA REDUCTION

Three systems that were assumed to be hosts of possible TDG candidates by Eigenthaler et al. (2015) were taken into account. TDGs are (physically) small objects, so their expected angular size is also rather small; no extended radio emission from them is likely to be revealed (unless radio data of subarcsecond resolution are used). As many of them form close to their host galaxies (Kaviraj et al. 2012), they are prone to be mistaken with other similar, but not self-gravitating entities, like e.g. H_{II} regions. Therefore, in order to prevent beam smearing of the emission from several entities into one, only loose-configuration, archive VLA data (at most B-configuration at 1.4 GHz, and C-configuration at 4.86 GHz) were chosen. Table 1 lists the basic information on the selected datasets.

All of the data used were imported into the Astronomical Image Processing System (AIPS) and calibrated following the standard continuum UV data calibration procedure. Final images were deconvolved using the CLEAN algorithm implemented in the task IMAGR, and corrected for the primary beam attenuation. Later on, the geometry of the maps of the Total Power (TP) radio

emission has been transformed using Everett interpolation to make it consistent with that of the cutouts from an optical sky survey using the task HGEOM, flux measurements were taken, and final images were created. In addition, NVSS data were also used to confirm if the possible detections – which were expected to be weak, thus possibly ambiguous – are represented also in the more sensitive, low-resolution map.

3. RESULTS

For each of the three systems studied, maps of the radio emission at 1.4, and 4.86 GHz were made. They are included in Fig. 1 (HCG 26), Fig. 3 (HCG 91), and Fig. 5 (HCG 96). Each of them is a three-image panel, with the upper part presenting the NVSS data, the middle – 1.4 GHz high-resolution archive data, and the bottom one – high-resolution archive data taken at 4.86 GHz. Area covered by the each of the radio maps was chosen in such a way that all of the TDG candidates are included. Throughout the paper, spatial distances were calculated according to Hickson et al. (1992).

First of the objects, HCG 26, is well visible in the NVSS, with an extension of the radio contour that encompasses all three TDG candidates (Fig. 1, upper panel). The 1.4 GHz archive data (Fig. 1, middle panel) show that most of this emission is likely to originate within the central galaxy, with only an isolated patch – barely exceeding the 3 r.m.s. level – located close to the TDG candidates. However, a close inspection (Fig. 2) reveals that the maximum of the radio emission at 1.4 GHz (0.34 ± 0.07 mJy) is displaced from the optical structure; the distance between the aforementioned patch and the closest candidate (HCG 26b) is comparable to the size of the telescope beam. At 4.86 GHz (Fig. 1, lower panel), none of the aforementioned structures is still visible. Therefore, it is concluded that the detected emission is not associated with any of the TDG candidates.

Datasets for the second group, HCG 91, are noticeably shorter in time (see Table 1); this is reflected in the highest noise level among all datasets at both L- (225 μ Jy/beam) and C-band (125 μ Jy/beam). HCG 91 has also the highest number of possible TDGs among those investigated in this study – 10. Out of this number, 4 are possible radio emitters: HCG 91c and HCG 91d are immersed in the same radio structure as their parent galaxies, while HCG 91i and HCG 91j share a common radio contour that does not connect to their mother galaxy (Fig. 3, upper panel). The higher resolution 1.4 GHz data (Fig. 3, middle panel) show that

Table 1. Basic information on the interferometric datasets used in this study.

HCG No.	L-band					C-band				
	Project	TOS [s]	Resolution	Noise [μ Jy/beam]	Conf.	Project	TOS [s]	Resolution	Noise [μ Jy/beam]	Conf.
26	AM344	930	$8.9'' \times 5.8''$	70	A/B	AM219	340	$1.8'' \times 1.6''$	30	C
91	AT149C	440	$12.8'' \times 8.1''$	250	B/C	AC345B	190	$8.3'' \times 3.4''$	125	C
96	AS267	1350	$5.4'' \times 4.3''$	120	B	AM219	350	$1.2'' \times 0.7''$	75	A

only HCG 91i seems to be a (point-source) radio emitter, with a flux density of 2.21 ± 0.23 mJy/beam. This source is still visible at 4.86 GHz (Fig. 3), where its flux density is equal to 0.72 ± 0.13 mJy/beam. Closer inspection (Fig. 4) reveals that both at 1.4, and 4.86 GHz, the radio contours perfectly match with the position of HCG 91i reported by [Egenthaler et al. \(2015\)](#), suggesting that it is, indeed, a radio-emitting TDG candidate.

In case of the last object in this study, HCG 96, the datasets are both the longest and have the highest resolution among the ones used in this study. The radio contours from the NVSS (Fig. 5, upper panel) encompass also the candidate HCG 91a, while HCG 91b is not enclosed. Archive data at both 1.4 (Fig. 5, middle panel), and 4.86 GHz (Fig. 5, lower panel) show no emission outside of the parent galaxies.

4. DISCUSSION

As most of the relations regarding star formation used in the literature data relevant for this work have been calculated under the assumption of a Salpeter Initial Mass Function (IMF, [Salpeter 1955](#)), this IMF was adopted for all the measurements presented in this paper. In particular, the equations provided by [Murphy et al. \(2011\)](#), which use the Kroupa IMF ([Kroupa 2001](#)), where re-calibrated by introducing a factor of 1.6, as outlined by [Calzetti et al. \(2007\)](#). Common values for the distances to the sources relevant for this study were also adopted, and all values dependant on them were re-calculated.

4.1. What is the origin of the radio emission?

Analysis of the archive data suggests that among the TDG candidates from HCG 26, HCG 91, and HCG 96, only HCG 91i is visible at 1.4 and 4.86 GHz. In order to extract the exact coordinates of the radio source, the AIPS task IMFIT was used. The derived positions, as well as the position of the H_α emitter associated with HCG 91i given by [Egenthaler et al. \(2015\)](#) are presented in Table 2. It turns out that the offset between the fitted maxima of radio emission at 1.4 and 4.86 GHz is equal to

$1.2''$. The theoretical precision (returned by the IMFIT task) is around $0.6''$, so this displacement is not worrying – moreover, as the beam size at each of the frequencies is larger, it is in fact negligible. The exact distance between the detection at 4.86 GHz (where the resolution is higher) and the position estimated from H_α data is even lower – $0.3''$. Assuming that the whole system is located approximately 101 Mpc away ([Hickson et al. 1992](#)), this translates into a physical separation of less than 150 pc. HCG 91j, the other nearby TDG candidate, is located as far as $11.3''$ – a distance larger than the size of the beam at 4.86 GHz. This altogether suggests that if the radio emission is intrinsic to any of the TDG candidates, then HCG 91i would be its most probable host.

Table 2. Positions of the radio and H_α sources associated with HCG 91i.

Data	α (J2000.0)	δ (J2000.0)
H_α^1	$22^h 09^m 06.98^s$	$-27^\circ 46' 42.4''$
1.4 GHz	$22^h 09^m 06.95^s$	$-27^\circ 46' 43.0''$
4.8 GHz	$22^h 09^m 07.00^s$	$-27^\circ 46' 42.2''$

1) From [Egenthaler et al. \(2015\)](#)

While HCG 91i is the single detected radio source among all of the TDG candidates studied, it is not the most luminous one in the H_α line ([Egenthaler et al. 2015](#)). HCG 91c, HCG 91d, HCG 91e, and HCG 91j have all higher H_α luminosity, while HCG 91a and HCG 91g are similar to the detected TDGc in this regard. As the H_α star formation rate (SFR_{H_α}) is proportional to the H_α luminosity ([Murphy et al. 2011](#)), the most luminous object should also be the most actively star forming one. Moreover, the 1.4 GHz emission can also be used as an estimator of the SFR ([Condon et al. 2002](#); [Murphy et al. 2011](#); [Heesen et al. 2014](#)), so it is possible both to estimate the expected 1.4 GHz luminosity, and the 1.4 GHz-derived SFR ($SFR_{1.4\text{GHz}}$) – and compare these values to each other. In order to calculate $SFR_{1.4\text{GHz}}$ and to estimate the expected radio flux at that frequency, Equa-

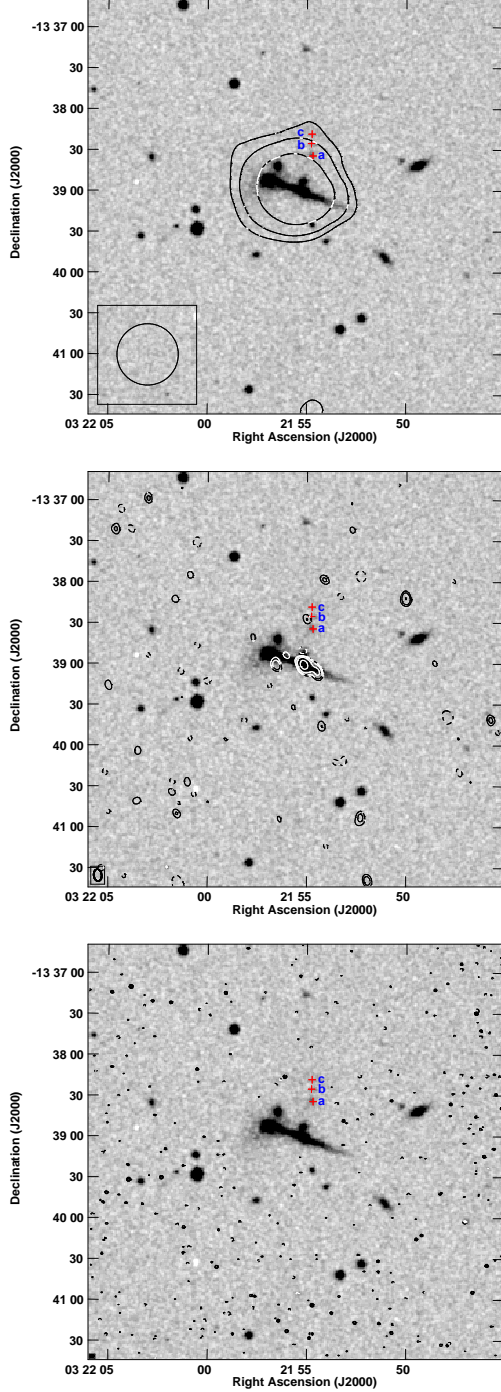


Figure 1. Maps of the radio emission of HCG 26. Radio contours overlaid on a POSS-II Johnson-R filter map. The levels are 3, 5, 10, 25, 50 \times r.m.s. noise level. **Upper panel:** NVSS map; r.m.s. noise level of 450 μ Jy/beam, angular resolution of $45'' \times 45''$. **Middle panel:** 1.4 GHz emission; r.m.s. noise level of 70 μ Jy/beam, angular resolution of $8.9'' \times 5.8''$. **Lower panel:** 4.86 GHz emission; r.m.s. noise level of 30 μ Jy/beam, angular resolution of $1.8'' \times 1.6''$.

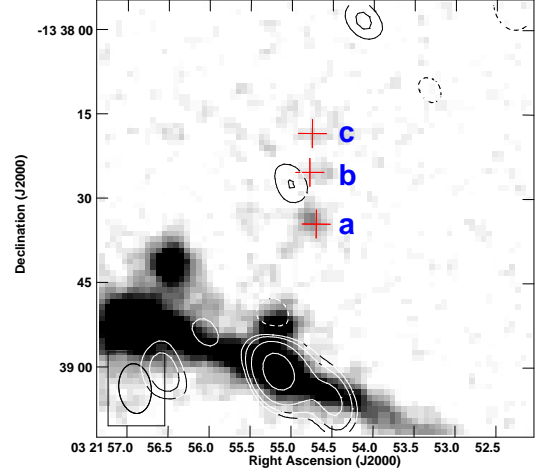


Figure 2. Map of the radio emission of HCG 26 at 1.4 GHz in the vicinity of TDG candidates **a**, **b**, and **c**. Radio contours overlaid on a (high-contrast) cutout of the POSS-II Johnson-R filter map. The levels are 3, 5, 10, 25 \times r.m.s. noise level of 70 μ Jy. The angular resolution is $8.9'' \times 5.8''$.

tion (17) from [Murphy et al. \(2011\)](#), re-calibrated to the Salpeter IMF ([Salpeter 1955](#)), connecting the radio luminosity and star formation rate was used:

$$\left(\frac{\text{SFR}_{1.4\text{GHz}}}{M_{\odot}\text{yr}^{-1}} \right) = 1.02 \times 10^{-28} \left(\frac{L_{1.4\text{GHz}}}{\text{ergs}^{-1}\text{Hz}^{-1}} \right) \quad (1)$$

Substituting $L_{1.4\text{GHz}} = 4\pi d^2 S_{1.4\text{GHz}}$, where d is the distance to the source, and expressing $S_{1.4\text{GHz}}$ in [Jy], and d in [Mpc], this equation takes the following form:

$$\left(\frac{\text{SFR}_{1.4\text{GHz}}}{M_{\odot}\text{yr}^{-1}} \right) = 1.22 \times 10^{-1} \left(\frac{S_{1.4\text{GHz}} \cdot d^2}{\text{Jy Mpc}} \right) \quad (2)$$

To estimate the radio flux from $\text{SFR}_{\text{H}\alpha}$, this can be transformed into:

$$\left(\frac{S_{1.4\text{GHz}}}{\text{Jy}} \right) = 13.08 \left(\frac{\text{SFR}_{\text{H}\alpha} \cdot d^{-2}}{M_{\odot}\text{yr}^{-1}\text{Mpc}^{-2}} \right) \quad (3)$$

Equations 2 and 3 were then used to calculate the expected SFR/upper constraints from the radio flux/3 r.m.s. noise level, and vice versa. Apart from the detected HCG 91i, the most $\text{H}\alpha$ -luminous TDG candidates in each of the systems were used. Results can be seen in Table 3. It turns out, that *none* of the TDG candidates should be detected at 1.4 GHz! The radio flux extrapolated from the $\text{H}\alpha$ data for most of these objects should not exceed a few μ Jy in most of the cases – thus being undetectable using the currently available radio

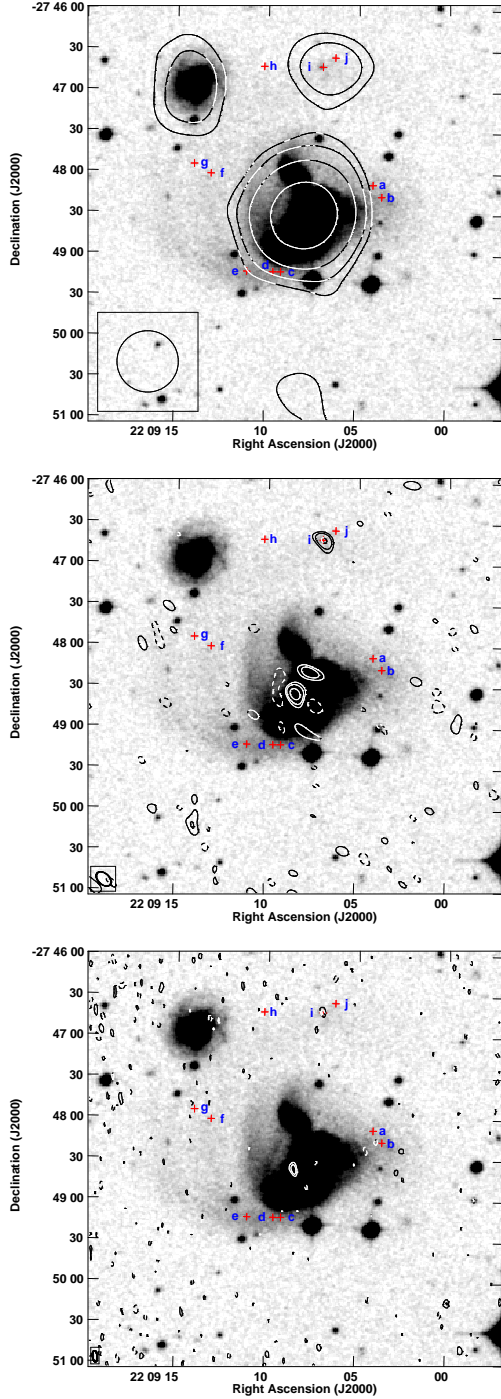


Figure 3. Maps of the radio emission of HCG 91. Radio contours overlaid on a POSS-II Johnson-R filter map. The levels are 3, 5, 10, 25, 50 \times r.m.s. noise level. **Upper panel:** NVSS map; r.m.s. noise level of 450 μ Jy/beam, angular resolution of $45'' \times 45''$. **Middle panel:** 1.4 GHz emission; r.m.s. noise level of 250 μ Jy/beam, angular resolution of $12.8'' \times 8.1''$. **Lower panel:** 4.86 GHz emission; r.m.s. noise level of 125 μ Jy/beam, angular resolution of $8.3'' \times 3.4''$.

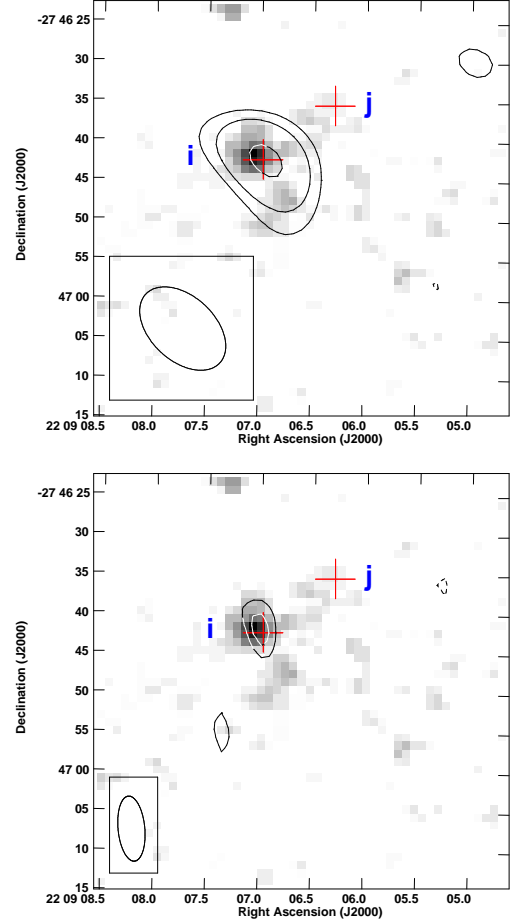


Figure 4. Maps of the radio emission of HCG 91 in the vicinity of TDG candidates i and j. Radio contours overlaid on a (high-contrast) cutout of the POSS-II Johnson's red map. The levels are 3, 5, 10 \times r.m.s. noise level. **Top:** 1.4 GHz emission; r.m.s. noise level of 250 μ Jy/beam, angular resolution of $12.8'' \times 8.1''$. **Bottom:** 4.86 GHz emission; r.m.s. noise level of 125 μ Jy/beam, angular resolution of $8.3'' \times 3.4''$.

data. The radio upper limits for the SFR of the non-detected TDGs are approximately two orders of magnitude higher, than that from Eigenthaler et al. (2015). The same conclusion is derived when using equation 21 from Condon et al. (1992): assuming a spectral index of 0.8, none of the TDG candidates has an expected radio flux higher than approximately 50 μ Jy. Such a discrepancy raises doubts if the radio emission is indeed connected to the TDG candidate; another, straightforward explanation might be that it originates in a background radio source, which is just by chance so angularly close to the H_α maximum associated with HCG 91i. Therefore, a series of different tests have been carried out, all of them presented in paragraphs below. To avoid excessive usage of terms like "radio emission", "radio source"

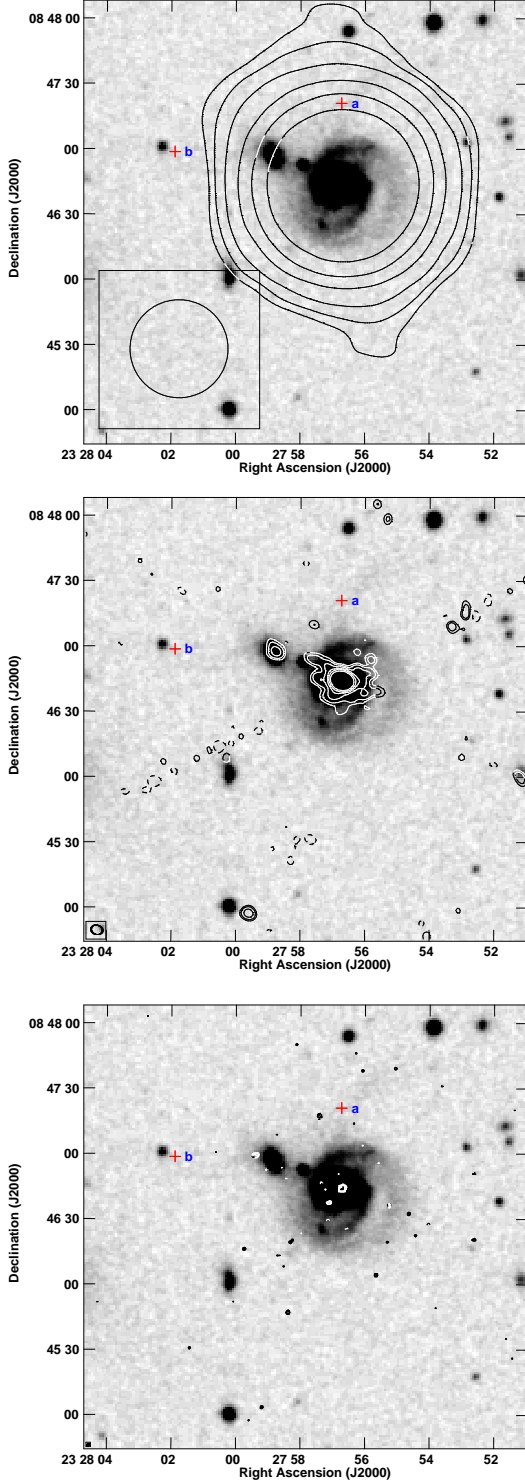


Figure 5. Maps of the radio emission of HCG 96. Radio contours overlaid on a POSS-II Johnson's red map. The levels are 3, 5, 10, 25, $50 \times$ r.m.s. noise level. **Upper panel:** NVSS map; r.m.s. noise level of $450 \mu\text{Jy}$, angular resolution of $45'' \times 45''$. **Middle:** 1.4 GHz emission; r.m.s. noise level of $120 \mu\text{Jy}$, angular resolution of $5.4'' \times 4.3''$. **Bottom:** 4.86 GHz emission; r.m.s. noise level of $90 \mu\text{Jy}$, angular resolution of $1.2'' \times 0.7''$.

etc. the designation HCG 91RS will be used from now on to name the radio counterpart.

Table 3. Radio flux density, its extrapolation from the $\text{H}\alpha$ luminosity, and a comparison between the 1.4 GHz, and $\text{H}\alpha$ -derived SFR for HCG 91i and three non-detected TDG candidates

Object	$S_{1.4\text{GHz}}$ μJy	$S_{1.4\text{GHz,est.}}$ μJy	$\log(\text{SFR}_{1.4\text{GHz}})$ $M_{\odot}\text{yr}^{-1}$	$\log(\text{SFR}_{\text{H}\alpha})$ $M_{\odot}\text{yr}^{-1}$
HCG 91i	2210	7.3	0.41	-2.27
HCG 91d	<675	15.7	<-0.08	-1.94
HCG 26a	<150	2.8	<-0.47	-2.45
HCG 96a	<360	1.5	<-0.08	-2.77

4.2. Radio spectrum of HCG 91RS

A possibility that HCG 91RS is just an imaging artefact would be one of the most straightforward explanations. However, the detection was made at two separate observing bands; moreover, at the L-band, observations were carried out using two different configurations of the VLA. As a result, the point spread functions of each of the datasets are different, so emergence of an artefact at the same sky position is unlikely. The flux densities of HCG 91RS derived both from the NVSS and the high resolution data are also coherent. Therefore, this scenario seems not to be a probable one.

Additional information on the nature of a radio source can be derived from its radio spectrum. Unfortunately, HCG 91RS is not an easy target for such a study: it has a relatively steep spectrum, which hinders efforts to detect it at higher frequencies (especially as it is a rather weak emitter). In addition, in order to avoid smearing its signal with the emission from the central galaxy of HCG 91, high resolution observations are desirable. The NRAO Data Archive lists one possibly useful dataset – recorded at 8.46 GHz. Assuming the same spectral index as between L- and C-bands – 0.91 ± 0.21 ($\alpha \propto \nu^{-\alpha}$) – HCG 91RS should have a flux density of $0.45 \pm 0.13 \text{ mJy}$ at 8.46 GHz – detectable at at least 5 r.m.s. level. However, this is not the case; either HCG 91i is extended at the angular scales larger than that of the beam (which is 0.5 arcsec in this case) and the resolved parts are too weak to be detected, or its spectrum steepens even further between 4.86 and 8.46 GHz – the flattest slope to imply a lack of detection at the given 3 r.m.s level is 1.41.

HCG 91i can be looked upon at the lower frequencies, too – in the TGSS ADR (Intema et al. 2016) survey;

this data were collected at 150 MHz, have an angular resolution of $25''$ on $25'' \times \sec(-19^\circ)$, but come with a limited sensitivity to extended structures. Assuming a 1420 MHz flux density of HCG 91RS of 2.24 ± 0.23 mJy, and once again, $\alpha = 0.91 \pm 0.21$, one can expect the 150 MHz flux density to be around 20 mJy; this is, at a $13 \times$ r.m.s. level. However, similarly to the 8.46 GHz data, this is not the case. The TGSS ADR map (see Fig. 6) reveals emission from the central pair of galaxies only. If the $3 \times$ r.m.s. level is substituted to calculate the spectral index between 150 MHz and 1.4 GHz, then the resulting value is equal to 0.31 ± 0.06 . This would indicate a very flat spectrum, reaching the flatness limit for the non-thermal radio spectra (Weiler & Sramek 1988). As a result, either the radio spectrum steepens significantly in the supra-GHz regime, but is relatively flat at lower frequencies, or the low frequency flux density is underestimated.

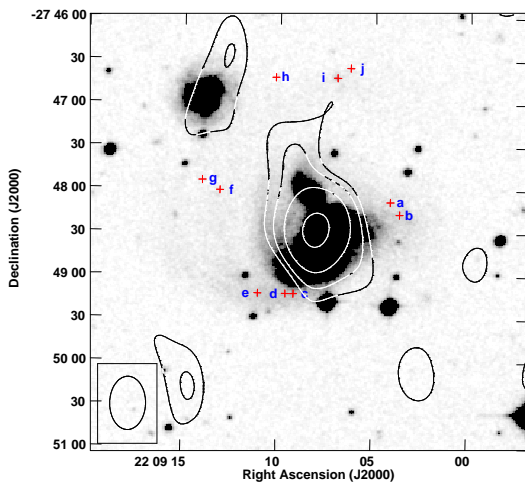


Figure 6. Map of the radio emission of HCG 91 at 150 MHz. TGSS radio contours overlaid on a (high-contrast) cutout of the POSS-II Johnson-R filter map. The levels are 3, 5, 10, $25 \times$ r.m.s. noise level of 1.5 mJy. The angular resolution is $38.8'' \times 25''$.

Gathering the radio information altogether, there are two likely explanations for the spectrum of HCG 91RS. If it is a background radio galaxy, it is a somewhat older object, with a spectrum quickly steepening around 1 GHz, or an example of a Gigahertz-Peaked Source O’Dea et al. (1991). If the emission indeed comes from HCG 91i, then the possible mechanism responsible for the low frequency flattening could be the absorption of the synchrotron radiation on the thermal electrons in the source itself – a process that is expected to take place in the star-forming regions. With TDG candidates be-

ing in fact detached, self-gravitating regions of excessive star formation – and given the estimated $\text{SFR}_{1.4\text{GHz}}$ for HCG 91RS – this could explain the lack of detection at 150 MHz. Similar situation happens for the TDG candidate SQ-B from HCG 92: assuming the flux density and spectral index provided by Nikiel-Wroczyński et al. (2013b), one could expect it to be detectable in the TGSS, which is not the case. At the higher frequency, the lack of the detection of HCG 91i can be attributed to the over-resolving of the source’s structure: the 0.5-arcsec resolution of the set translates into a physical scale of around 250 pc – smaller than the typical size of a TDG candidate.

4.3. Dust attenuation

Given the fact that in case of HCG 91i and 91RS it is the $\text{SFR}_{\text{H}\alpha}$ that is much lower than $\text{SFR}_{1.4\text{GHz}}$, a possible explanation for the mismatch between these two indicators could be the extinction of $\text{H}\alpha$ flux on dust grains. This effect can be significant, and usually can be corrected for by using either the 22, 24 or the 25 μm data (see eg. Calzetti et al. 2007; Murphy et al. 2011; Kennicutt & Evans 2012). It would be even more plausible reason given the fact that HCG 91i is located at the tip of a tidal arm/tail – such TDGs are prone to accumulate larger amounts of matter, including dust (Bournaud 2004). There is no direct detection of 22 μm emission from HCG 91i in the WISE data, but some upper constraints can still be derived. Assuming an upper flux constraint of ≈ 2.3 mJy calculated from the catalogue data on the magnitudes of the sources of interest following the instructions provided in the *Explanatory Supplement to the WISE Preliminary Data Release Products*¹ and using Equations 6 and 7 from Murphy et al. (2011) (re-calibrated into the Salpeter IMF), one arrives at $\text{SFR}_{\text{H}\alpha, \text{corr}} = 0.1 \text{ M}_{\odot} \text{ yr}^{-1}$. This value is more than an order of magnitude higher than the non-corrected $\text{SFR}_{\text{H}\alpha}$ from Eigenthaler et al. (2015); however, this is the theoretical maximal expected flux, and yet it is still about an order of magnitude lower, than $\text{SFR}_{1.4\text{GHz}}$. Therefore, dust extinction of $\text{H}\alpha$ flux solely can’t explain the observed discrepancy.

4.4. Typical discrepancies between $\text{SFR}_{1.4\text{GHz}}$ and $\text{SFR}_{\text{H}\alpha}$ for starbursting dwarf galaxies

The most challenging issue in linking HCG 91i to HCG 91RS is the discrepancy between its $\text{SFR}_{1.4\text{GHz}}$ and $\text{SFR}_{\text{H}\alpha}$. To investigate if such a situation can be regarded as a typical one, I have used Eq. 2 for a subset of nearby starbursting dwarf galaxies from

¹ http://wise2.ipac.caltech.edu/docs/release/prelim/expsup/wise_prelrel_toc.

McQuinn et al. (2010) for which the 1.4 GHz NVSS data (Condon et al. 1998) were available. To supplement this sample, two TDG candidates SQ-A and SQ-B were added. Distances were taken from the NASA Extragalactic Database (except for SQ-A and SQ-B, where Hickson et al. 1992 estimates were used). All of these objects are small galaxies, most of them have a diameter lower than 3 kpc (larger sizes of TDG candidates might arise from a less precise measurement). Results can be seen in Table 4. It turns out that in general, those star-bursting dwarf galaxies that have significant 1.4 GHz flux have $\text{SFR}_{1.4\text{GHz}}$ in agreement with $\text{SFR}_{\text{H}\alpha}$. Several objects have their radio estimates about an order of magnitude lower, than that from $\text{H}\alpha$; however, these are all relatively weak objects (in both regimes). In addition, NGC 625 and NGC 2366 are the smallest ones considered in this sample. As a result, uncertainties in radio flux can easily lead to a large mismatch between calculated SFRs.

In case of SQ-A and SQ-B, the radio data have much higher resolution and sensitivity – hence, it should be possible to avoid such uncertainties. However, while for SQ-B both SFR estimates are in a nearly perfect agreement, that does not happen in the case of SQ-A. Here the $\text{SFR}_{\text{H}\alpha}$ is very high; more than two times higher than the estimated $\text{SFR}_{1.4\text{GHz}}$. Even more interestingly, the tendency observed for HCG 91i and HCG 91RS is reversed: for SQ-A it is the $\text{SFR}_{\text{H}\alpha}$ measurement (dust-corrected), that is much higher than the radio one. Unfortunately, the lack of other known radio-emitting TDG candidates renders it impossible to investigate if discrepancies between radio and $\text{H}\alpha$ estimators are a common occurrence. Nevertheless, none of the comparison objects shows as large difference between these two estimators as HCG 91i and HCG 91RS do.

4.5. Stellar content and $\text{SFR}-M_*$

Not only is there a large discrepancy between $\text{SFR}_{1.4\text{GHz}}$ and $\text{SFR}_{\text{H}\alpha}$, but also the very value of radio SFR seems to be unrealistically high: objects listed by Lisenfeld et al. (2016) exhibit star formation rates of $0.005 - 0.32 \text{ M}_\odot \text{ yr}^{-1}$, so at least an order of magnitude lower than $\text{SFR}_{1.4\text{GHz}} = 2.6 \text{ M}_\odot \text{ yr}^{-1}$ for HCG 91RS. However, there are at least two known examples of TDG candidates with a relatively high SFR, namely SQ-A and SQ-B regions present in HCG 92. In order to use a consistent distance estimate for all the derivations carried out in this study, I have recalculated the $\text{SFR}_{\text{H}\alpha}$ provided by Xu et al. (2003) for SQ-A and Lisenfeld et al. (2016) for SQ-B, arriving at 1.84 and $0.57 \text{ M}_\odot \text{ yr}^{-1}$, respectively. It is then feasible to test if such values would be reliable, eg. by comparing the

Table 4. $\text{SFR}_{1.4\text{GHz}}$ for a subset of starburst dwarf galaxies derived from the NVSS catalogue and compared to $\text{SFR}_{\text{H}\alpha}$ from McQuinn et al. (2010)

Object	$\frac{d}{\text{Mpc}}^1$	$\frac{D}{\text{kpc}}$	$\frac{S_{1.4\text{GHz}}}{\text{mJy}}$	$\frac{\text{SFR}_{\text{H}\alpha}}{\text{M}_\odot \text{ yr}^{-1}}$	$\frac{\text{SFR}_{1.4\text{GHz}}}{\text{M}_\odot \text{ yr}^{-1}}$
HCG 91i/RS ²	98	3.15	2.2	<0.1	2.56
IC 4662	4.4	1.37	40	0.08	0.09
NGC 625	2.8	0.87	10	0.04	0.01
NGC 784	5.0	1.55	3	0.12	0.01
NGC 1569	3.4	1.06	362	0.24	0.51
NGC 2366	1.5	0.47	20	0.16	0.01
NGC 4214	7.5	2.34	38	0.13	0.26
NGC 4449	5.8	1.81	270	0.97	1.11
NGC 5253	9.3	2.90	86	0.40	0.91
SQ-A ³	90	3.59	0.8	1.84	0.79
SQ-B ⁴	90	3.32	0.6	0.57	0.59

¹ Diameter derived from *logd25* parameter from Makarov et al. (2014) (if not stated otherwise);

² Radio flux taken from this work, $\text{SFR}_{\text{H}\alpha}$ taken from Eigenthaler et al. (2015), recalculated using consistent distance estimate, and corrected for the maximal dust contamination, optical diameter roughly estimated using the background DSS map;

³ Radio flux taken from Xu et al. (2003), $\text{SFR}_{\text{H}\alpha}$ taken from Xu et al. (2003) and recalculated using consistent distance estimate, optical diameter roughly estimated using the WISE Band 1 data;

⁴ Radio flux taken from Xu et al. (2003), $\text{SFR}_{\text{H}\alpha}$ taken from Lisenfeld et al. (2016) and recalculated using consistent distance estimate, and re-calibrated from Kroupa to Salpeter IMF, optical diameter roughly estimated using the WISE Band 1 data.

derived SFR to the stellar content of these objects. In order to do so, I have used the WISE 3.6 and $4.5 \mu\text{m}$ data for all three objects and calculated the stellar content using the following relation from Eskew et al. (2012). The infrared fluxes were calculated using the same instructions as in 4.3:

$$\left(\frac{M_*}{\text{M}_\odot}\right) = 10^{5.65} \left(\frac{(F_{3.6\mu\text{m}})^{2.85}}{\text{Jy}}\right) \left(\frac{(F_{4.5\mu\text{m}})^{-1.85}}{\text{Jy}}\right) \left(\frac{20 \times D}{\text{Mpc}}\right)^2 \quad (4)$$

This yields stellar masses equal to $10^{9.04} \text{ M}_\odot$ for HCG 91i, $10^{9.37} \text{ M}_\odot$ for SQ-A, and $10^{8.58} \text{ M}_\odot$ for SQ-B. This in turn identifies SQ-A and HCG 91i as relatively massive TDG candidates, as the statistical study of Kaviraj et al. (2012) shows that an average stellar mass of such an object varies between $10^{8.2}$ and $10^{8.4} \text{ M}_\odot$,

depending on its location (at the base/along/ at the tip of the tidal tail). These values were then substituted to the SFR–mass relation for late type galaxies given by Calvi et al. (2018). The range of expected SFR (in $M_{\odot}\text{yr}^{-1}$) is 0.2–1.3 for HCG 91i, 0.3–1.6 for SQ–A, and 0.1–0.6 for SQ–B. In case of SQ–A and SQ–B, it is in a good agreement with both $\text{SFR}_{1.4\text{GHz}}$ and $\text{SFR}_{\text{H}\alpha}$; the $\text{SFR}_{\text{H}\alpha}$ estimate for the former one is a bit larger than the expected value. Contrary to that, for HCG 91i, only one SFR indicator can be assumed to be similar to the predictions based on the the stellar mass – the radio one, albeit the derived SFR is nearly twice as much as the expected one. On the other hand, $\text{SFR}_{\text{H}\alpha}$ for HCG 91i, even after correcting for the dust contamination, is more than an order of magnitude lower, than what one would expect from the SFR– M_{\star} relation. As a result, not only is the star formation rate as high as the estimated $\text{SFR}_{1.4\text{GHz}}$ feasible, but it turns out to be the one fitting better to the SFR– M_{\star} relation.

4.6. Variations in the SFR over the time

Another explanation of the discrepancy between $\text{SFR}_{1.4\text{GHz}}$ and $\text{SFR}_{\text{H}\alpha}$ could be a series of star formation bursts inside HCG 91i. SFR estimators are sensitive to stars of different age: as outlined by Kennicutt & Evans (2012), for the $\text{H}\alpha$ estimator the mean age of the stars that contribute to the emission is around 3 Myrs, and 90% of emission comes from the ones that are younger than 10 Myrs. Other estimators are sensitive to different populations: for example, the ultraviolet tracer is sensitive to the population which has a mean age of 10 Myrs, and the age range of the objects that contribute to this emission is much larger, than in the case of $\text{H}\alpha$: it is 100 Myrs for the far- and 200 Myrs for the near-ultraviolet light. In case of the 1.4 GHz emission, the mean age is equal to 100 Myrs – and the “boundary” age is even not estimated. Series of subsequent bursts could result in an enhanced magnetic field/radio emission, suggesting a still high SFR, while the most current value, traced by the $\text{H}\alpha$ emission would be lower, if the object under consideration is in a more quiescent phase. If this is indeed the case of HCG 91i, then it should still be a strong UV emitter. In order to evaluate this scenario, I have checked the GALEX FUV and NUV maps. The results are not encouraging: first of all, there is no UV source that could be directly associated with HCG 91i. The closest ones are very faint (NUV fluxes of less than $15\mu\text{Jy}$), and only one of them was detected in both FUV and NUV. The distance between them and the radio maximum is significant – more than 10 arcseconds, so at least 4.5 kpc – more than the expected size of the whole TDG candidate. I have estimated the SFR using

the relations presented by Kennicutt & Evans (2012), derived from the earlier works of Hao et al. (2011) and Murphy et al. (2011), and recalibrated for the Salpeter IMF. The FUV and NUV fluxes were taken for the nearest source detected in both of these bands, and corrected for the dust extinction using the WISE Band 4 upper flux limit of 2.3 mJy. The dust-enshrouded SFR_{FUV} is equal to approximately $0.03M_{\odot}\text{yr}^{-1}$, and SFR_{NUV} is approximately $0.04M_{\odot}\text{yr}^{-1}$. These values are lower than those estimated for the dust-enshrouded $\text{SFR}_{\text{H}\alpha}$ (and thus, much lower than the $\text{SFR}_{1.4\text{GHz}}$). Therefore, the hypothesis of subsequent burst can be safely discarded.

4.7. An inherited magnetic field?

One of the most fundamental differences between the $\text{SFR}_{1.4\text{GHz}}$ and $\text{SFR}_{\text{H}\alpha}$ estimators is the evolutionary stage of the objects they probe. The latter one relies on the presence of an ionised gas surrounding a young, massive star. Contrary to that, the radio one is aimed at a much older ones: it is, in fact, a *post mortem* survey, as the synchrotron emission relies on the relativistic electrons supplied by the supernovae. Traces of these processes fade away on different timescales: radio emission can still be detectable tens of Myrs after last electrons where supplied. Therefore, one can propose a hypothesis that while both the radio and $\text{H}\alpha$ emission are connected to HCG 91i, only the latter one is caused by processes intrinsic to (or triggered inside) this object. Majority of the radio emission is caused by an electron population supplied to the magnetic field when what is now regarded as a TDG candidate was still a part of its parent object. Analysis of the radio spectrum of HCG 91RS seems to be consistent with this scenario. With a spectral index of 0.91 ± 0.21 , it is a rather steep (thus aged) one. Young supernovae remnants have in general much flatter indices: the lower limit is assumed to be equal to 0.3 (Weiler & Sramek 1988). Such flat spectra are indeed seen in case of disk star forming regions – like it happens in case of the dwarf starburst galaxy pair Arp 269 (Nikiel-Wroczyński et al. 2016). A rough estimate of the spectral age, made under the assumption that the break frequency of the spectrum is already below 4.86 GHz suggests that the radio emission must be older than approximately 10–15 Myrs – likely more. In addition, the aforementioned scenario easily explains the excessive strength of the magnetic field associated with HCG 91RS (see Sect. 4.8). The obtained value of 11–16 μG is, as already mentioned, similar to that of example disk star forming regions. If HCG 91i began its life as a region of vigorous star formation inside the spiral arm of HCG 91A and was later separated due to the

action of tidal forces, then a strong, "remnant" magnetic field would be indeed expected. While at the first glance the scenario where HCG 91i and HCG 91RS are the same object, but their emission represents fundamentally different moments in its past seems to be able to easily explain the observed discrepancies, it also has several important caveats. There is neither information on the interaction history of the whole group, nor about the stellar population of HCG 91i. It is then impossible to address the problem quantitatively, eg. compare the spectral age with the expected time elapsed since the interaction started. Additional studies on HCG 91i and the history of the system as a whole are necessary to test the feasibility of this hypothesis.

An additional hint for the feasibility of the hypothesis described above comes from the analysis of optical maps: albeit there are four more H_α -luminous TDG candidates in their host system than HCG 91i, it is the only one luminous enough to be included in the USNO A-2.0 catalogue with an absolute magnitude in these filters of ≈ -16 , and the only one to be unambiguously detected in the infrared 3.6 and 4.5 μm data. Even in the background maps used for the radio images, it is the single TDG candidate with a clear optical counterpart. However, again there is a possibility that the observed object is just a superposition of a TDG candidate, and a distant background source.

Alas, the identification of HCG 91RS with HCG 91i remains ambiguous. Whereas there is neither a certain explanation for the discrepancy between $\text{SFR}_{1.4\text{GHz}}$ and SFR_{H_α} , nor the possibility of a background AGN galaxy can be ruled out fully, analysis of the stellar content and its relationship with the system's expected SFR clearly suggests that values similar to $\text{SFR}_{1.4\text{GHz}}$ would be expected. Additional data would be needed to prove, or disprove the hypothesis that HCG 91i is indeed another example of a rare, starbursting tidal dwarf galaxy candidate possessing a detectable magnetic field.

Last but not least, it is also worth to mention that many of the arguments presented in this study could be better assessed if there was a considerable literature data on radio emitting TDG candidates. With only three of such objects being known (assuming that HCG 91i is one of these), it is impossible to evaluate if any studied parameter can be considered typical (or not) for this class. A larger study aimed at revealing new radio-emitting TDG candidates is thus desirable.

4.8. Magnetic field inside the TDG candidates

If HCG 91RS is indeed the radio counterpart of HCG 91i, then it is possible to use the flux densities at 1.4 and 4.86 GHz to estimate the strength of its

magnetic field. The spectral index of 0.91 ± 0.21 was substituted into the BFELD code (Beck & Krause 2005) that calculates the basic properties of the magnetic field, together with a pathlength of 2000-4000 pc (similar to the size of the optical counterpart), and the proton-to-electron ratio of 100, which is believed to be maintained even in the starburst galaxies (Lacki & Beck 2013). The estimated magnetic field strength (under the assumption of equipartition of energy between the magnetic field and the cosmic rays) is then 11–16 μG . This is a strong magnetic field – stronger than the typical ones found for spiral galaxies by Niklas (1995), and approximately two times stronger than the one derived for the radio-emitting TDGc SQ-A and SQ-B (Nikiel-Wroczyński et al. 2013b). Such a strength is similar to that of the compact disk areas of star formation: Beck & Wielebinski (2013) lists several objects that host even stronger magnetic fields, and the study of the magnetic field of starburst dwarf spiral galaxy NGC 4490 (Nikiel-Wroczyński et al. 2016) reveals a handful of disk starburst regions hosting magnetic fields exceeding 20 μG in strength. Compared to the other dwarf galaxies, HCG 91i seems to possess a magnetic field similar to that of the starburst dwarf galaxies studied by Chyży et al. (2011).

While no detection was made in case of any other TDG candidate from the list of Eigenthaler et al. (2015), it is possible to estimate the upper constraints for the strength of magnetic field in these entities. Using the same pathlength as before, and calculating the spectral index using with the 3 r.m.s. levels of the respective radio data, it turns out that the magnetic fields of 6–8 μG strength can still remain undetected, due to high r.m.s noise levels. Such a value would also apply to HCG 91i, if the radio emission comes from a background source. A more sensitive study would allow to derive more strict constraints.

5. CONCLUSIONS

This work attempted to detect the radio counterparts of the Tidal Dwarf Galaxy (TDG) candidates in compact galaxy groups HCG 26, 91, and 96. On the basis of the gathered and analysed material, the conclusions are as follows:

1. There are clear signs of radio emission spatially coincident with the TDG candidate HCG 91i (emission maxima matched with less than 150 pc separation) detected in H_α line by Eigenthaler et al. (2015) both at 1.4, and 4.86 GHz. The detected emission has a steep spectrum, characterised by an index of 0.91 ± 0.21 ;

2. Analysis of the high resolution 8.46 GHz and TGSS-ADR 150 MHz radio data yields no radio detection, suggesting that either the radio source is a Gigahertz Peaked Source (or an aged AGN), or a star-forming region, weak at lower frequencies due to the absorption of synchrotron radiation on the thermal electrons, and over-resolved and thus too faint to be seen at 8.46 GHz;
3. Even after the H_α luminosity is corrected for the dust attenuation (using upper constraints as no detection was made at $22\ \mu\text{m}$), $\text{SFR}_{H_\alpha, \text{corr}}$ is about an order of magnitude lower than $\text{SFR}_{1.4\text{GHz}}$;
4. Comparison of $\text{SFR}_{1.4\text{GHz}}$ and SFR_{H_α} for a subset of starbursting dwarf galaxies shows that in most of the cases these two values are either concordant, or the difference can be attributed to the accuracy of the measurement, with the single exception of SQ-A tidal dwarf galaxy candidate, where SFR_{H_α} is significantly higher, than its $\text{SFR}_{1.4\text{GHz}}$ (and HCG 91i, if the radio emission is intrinsic to it);
5. Analysis of the stellar content and SFR versus stellar mass relation suggests that both HCG 91i and SQ-A are massive objects, and their expected SFR values are of the order of $1\text{M}_\odot\text{yr}^{-1}$; hence, in case of the former object, it is the radio estimate that seems to be more feasible;
6. Ultraviolet star formation rates, even when corrected for the dust attenuation, are very low, thus

ruling out the possibility that the discrepancy between different SFR indicators is due to a burst of star formation;

7. At the moment the scenario in which HCG 91i is a former star-forming region of its parent galaxy, with the radio emission being a remnant of this evolutionary stage, seems to fit the observations (and estimations) the best;
8. Should the radio emission originate in HCG 91i, then the derived strength of the magnetic field inside is $11\text{--}16\ \mu\text{G}$, similar to that found in starburst dwarf galaxies, or disk regions of vigorous star formation;
9. If this is not the case, then the upper constraints for the strength of the magnetic field inside all of the TDG candidates in the studied systems vary from $6\text{--}8\ \mu\text{G}$, leaving a possibility that strong magnetic fields can still be left undetected.

I would like to thank the anonymous referee for a number of comments and suggestions that helped to significantly improve this paper. I am also indebted to Krzysztof Chyży, Marek Jamroz and Marian Soida from the Astronomical Observatory of the Jagiellonian University for useful comments and suggestions that also helped to improve this paper.

REFERENCES

- Adelman-McCarthy, J. K., et al., 2007, *ApJS*, 175, 297
- Beck R., Krause M., 2005, *AN*, 326, 414
- Beck, R., Wielebinski, R., in: *Stars and Stellar Systems*, Vol. 5: Galactic Structure and Stellar Populations, ed. G. Gilmore, Springer, Berlin 2013
- Bournaud, F., Duc, P. -A., Amram, P., Combes, F., Gach, J. -L., 2004, 425, 813
- Bournaud, F., 2010, *Advances Astron.*, 2010
- Brinks, E., Duc, P.-A., Walter, F. 2004, *Recycling Intergalactic and Interstellar Matter (IAU Symp. 217)*, ed. P.-A. Duc, J. Braine, & E. Brinks (San Francisco, CA: ASP), 532
- Calvi, R., Vulcani, B., Poggianti, B. M., Moretti, M., Fritz, J., Fasano, G., 2018, *MNRAS*, 481, 3456
- Calzetti, D., et al., 2007, *ApJ*, 666, 870
- Chyży K. T., Beck R., Kohle S., Klein U., Urbanik M., 2000, *A&A*, 355, 128
- Chyży, K. T., Weżgowiec, M., Beck, R., Bomans, D. J., 2011, *A&A*, 529, 94
- Condon, J. J., 1992, *ARA&A*, 30, 575
- Condon J. J., Cotton W. D., Greisen E. W., Yin Q. F., Perley R. A., Taylor G. B., Broderick J. J., 1998, *ApJ*, 115, 1693
- Condon, J. J., Cotton, W. D., Broderick, J. J., 2002, *AJ*, 124, 675
- O’Dea, C. P., Baum, S. A., Stanghellini, C., 1991, *ApJ*, 380, 660
- Duc, P. -A., Braine, J., Lisenfeld, U., Brinks, E., Boquien, M. 2007, *A&A*, 475, 187
- Eigenhafer, P., Ploekinger, S., Verdugo, M., Ziegler, B., 2015, *MNRAS*, 451, 2793
- Eskew, M., Zaritsky, D., Meidt, S., 2012, *AJ*, 143, 139
- Hao, C.-N., Kennicutt, R. C., Johnson, B. D., Calzetti, D., Dale, D. A., Moustakas, J., 2011, *ApJ*, 741, 124

- Heesen, V., Brinks, E., Leroy, A. K., Heald, G., Braun, R., Bigiel, F., Beck, R., 2014, *AJ*, 147, 103
- Hickson, P., 1982, *ApJ*, 255, 382
- Hickson, P., Mendes de Oliveira, C., Huchra, J. P., et al. 1992, *ApJ*, 399, 353
- Hunsberger, S. D., Zaritsky, D., 1996, *ApJ*, 462, 50
- Intema, H. T., Jagannathan, P., Mooley, K. P., Frail, D. A., 2016, *A&A*, 598, 78
- Kaviraj, S., Darg, D., Lintott, C., Schawinski, K., Silk, J., 2012, *MNRAS*, 419, 70
- Kennicutt, R. C., Evans, N. J., 2012, *ARA&A*, 50, 531
- Kepley, A. A., Mühle, S., Everett, J., Zweibel, E. G., Wilcots, E. M., Klein, U., 2010, *ApJ*, 712, 536
- Kroupa, P. 2001, *MNRAS*, 322, 231
- Lacki, B. C., Beck, R., 2013, *MNRAS*, 430, 317
- Lisenfeld, U., Braine, J., Duc, P. A., Boquien, M., Brinks, E., Bournaud, F., Lelli, F., Charmandaris, V., 2016, *A&A*, 590, 92
- Makarov, D., Prugniel, P., Terekhova, N., Courtois, H., Vauglin, I., 2014, *A&A*, 570, 13
- Makarova, L. N. et al., 2002, *A&A*, 396, 473
- Mirabel, I. F., Dottori, H., Lutz, D., 1992, *A&A*, 256, 19
- McQuinn, K. et al., 2010, *ApJ*, 721, 297
- Murphy, E. J., et al., 2011, *ApJ*, 737, 67
- Nikiel-Wroczyński, B., Soida, M., Urbanik, M., Weżgowiec, M., Beck, R., Bomans, D. J., Adebahr, B., 2013, *A&A*, 553, 4
- Nikiel-Wroczyński, B., Soida, M., Urbanik, M., Beck, R., Bomans, D. J., 2013, *MNRAS*, 435, 149
- Nikiel-Wroczyński, B., Soida, M., Bomans, D. J., Urbanik, M., 2014, *ApJ*, 786, 144
- Nikiel-Wroczyński, B., Jamrozy, M., Soida, M., Urbanik, M., Knapik, J., 2016, *MNRAS*, 459, 683
- Niklas S., 1995, PhD thesis, University of Bonn
- Salpeter, E.E. 1955, *ApJ*, 121, 161
- Stéphan, È. J.-M., 1877, *MNRAS*, 37, 334
- Weiler, K. W., Sramek, R. A., 1988, *ARA&A*, 26, 295
- Weżgowiec, M., Soida, M., Bomans, D. J., 2012, *A&A*, 544, 113
- Xu C. K., Lu N., Condon J. J., Dopita M., Tuffs R. J., 2003, *ApJ*, 595, 665
- Zwicky, F., 1956, *Ergebnisse der Exakten Naturwissenschaften* 29, 344

All Authors and Affiliations

BŁAŻEJ NIKIEL-WROCZYŃSKI^{1, 2}

¹*Astronomical Observatory of the Jagiellonian University, ul. Orla 171, 30-244 Kraków, Poland*

²*Leiden Observatory, Leiden University, Oort Gebouw, PO Box 9513, NL-2300 RA Leiden, the Netherlands*